Physics and phenomenology (the ALICE and heavy-ion theory perspectives)

Larissa Bravina (Oslo), Konrad Tywoniuk (Bergen),
Alexander Rothkopf (Stavanger), Ionut Arsene (Oslo)

QGP properties using charmonium and beauty hadrons

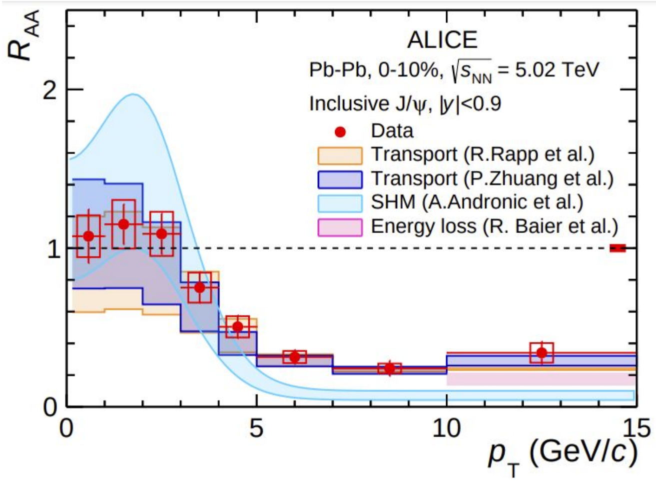

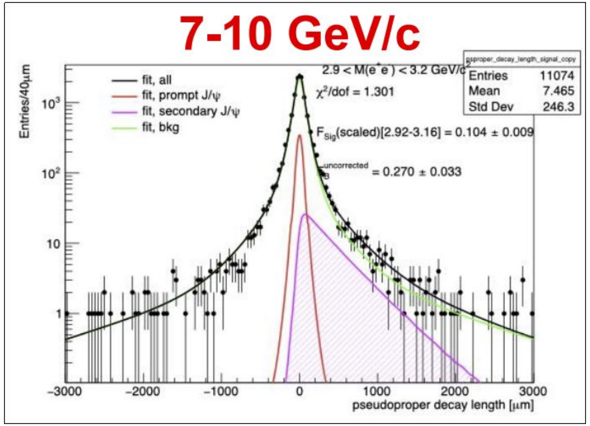

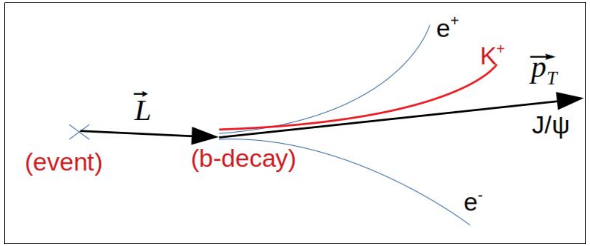

$B^+ \to J/\psi + K^+$

J/ψ measurements provides access to key measurements

- Charmonium production
- Beauty hadrons via non-prompt decays to J/ψ

Physics

- Modification of the QCD force in deconfined medium
- Thermalization of heavy quarks
- Flavor dependence of parton energy loss in QGP

Photoproduction in ultra-peripheral heavy-ion collisions

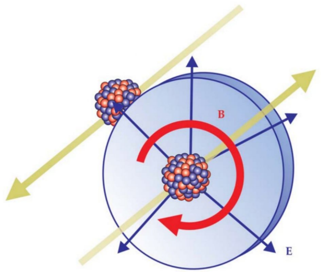

Nuclei interacting only via EM fields (B_{max} ~ 10^{15} T)

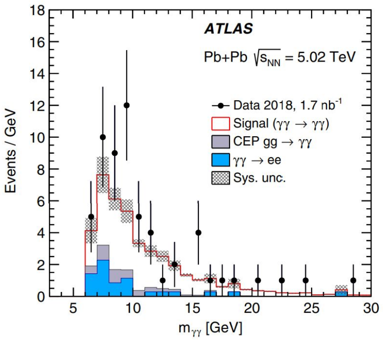

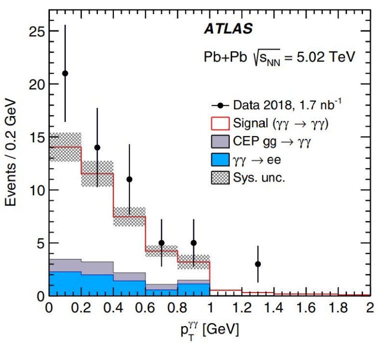

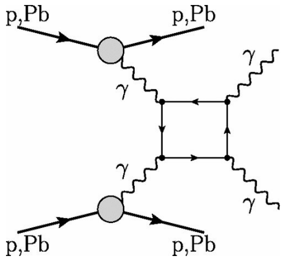

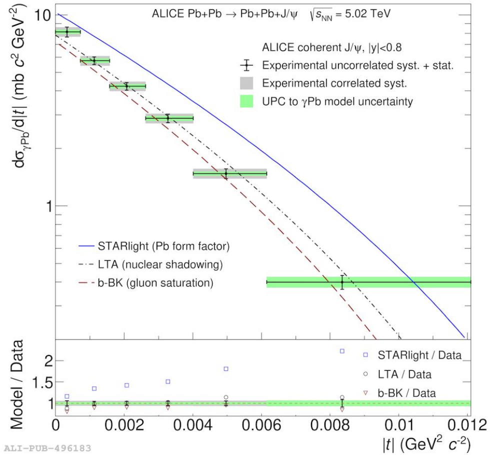

- Photo-production of vector mesons in ultra-peripheral collisions
  - sensitive to gluon density at low-x
- Light-by-light scattering
  - test for the Standard Model, sensitive to BSM physics

Nuclear gluon PDFs and gluon saturation (with ALICE FOCAL)

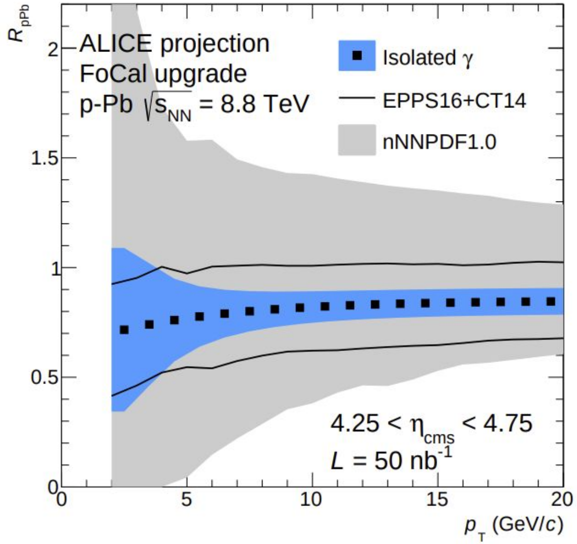

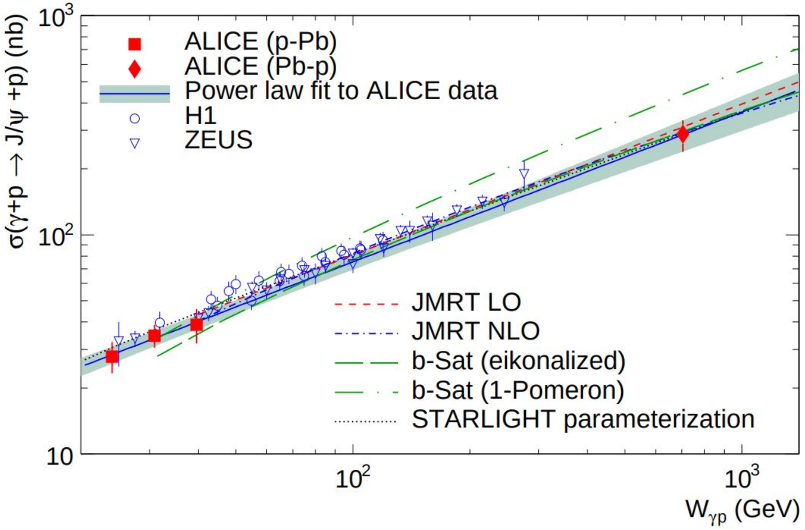

- Forward production of isolated photons
- Forward J/ψ photo-production in ultra-peripheral collisions

J/psi production in jets

ALICE - work in progress

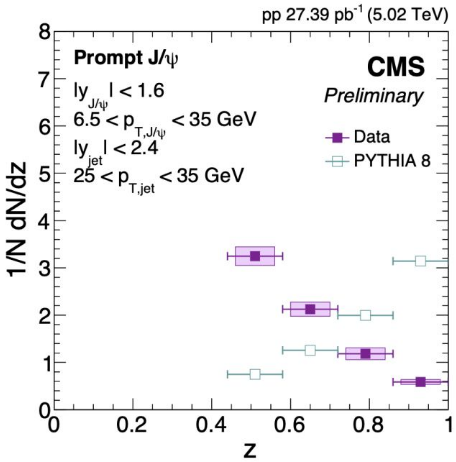

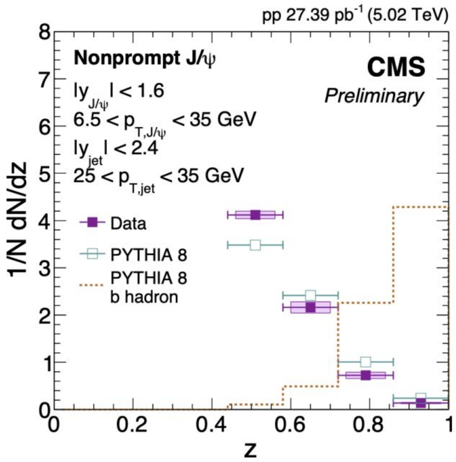

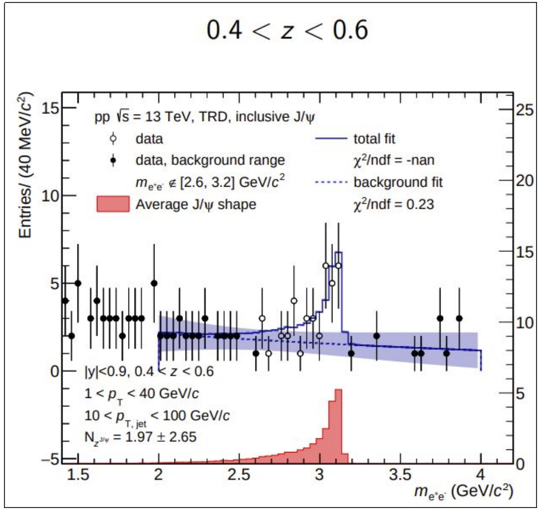

- Non-prompt J/psi tagged jets provide direct access to the beauty quark kinematics
  - Study parton flavor dependence of the QGP transport properties
- Prompt J/psi jets and their modification in QGP
  - Provide information on the mechanisms of J/psi nuclear suppression

High multiplicity pp collisions: multi-parton interactions and QGP

- Investigate multi-parton interactions phenomenology
- Onset of QGP in small systems using hard probes, i.e. open and hidden heavy flavor hadrons
    - existing measurements suggest final state effects in light flavor measurements
    - theoretically cleaner probes involving heavy flavor observables can be employed (so far suffer from large statistical uncertainties)

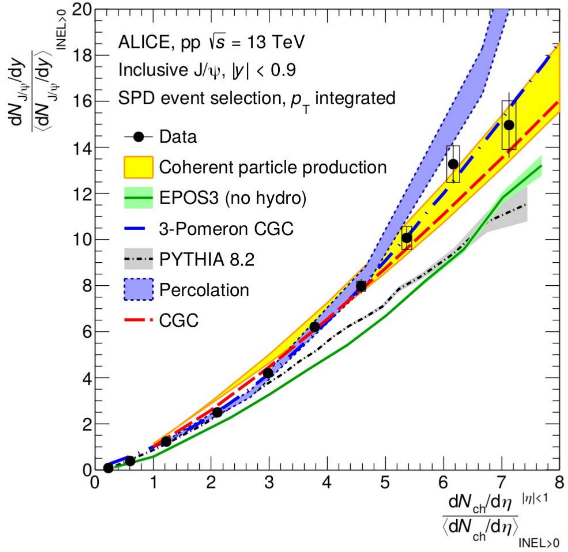

Nature of the X(3872)

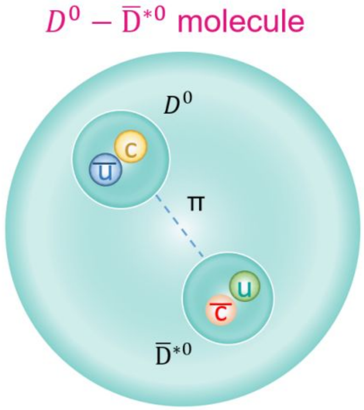

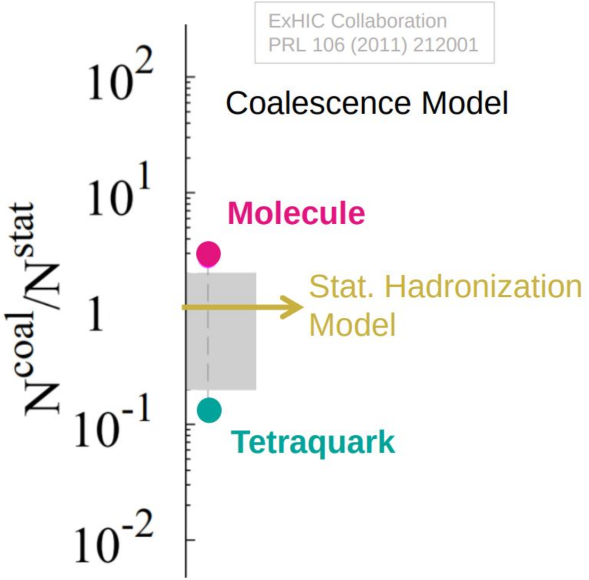

Nuclear suppression pattern of X(3872) is thought to be sensitive to its internal structure (strongly bound tetraquark or a D meson molecule)

Heavy-ion theory: jets and hard probes

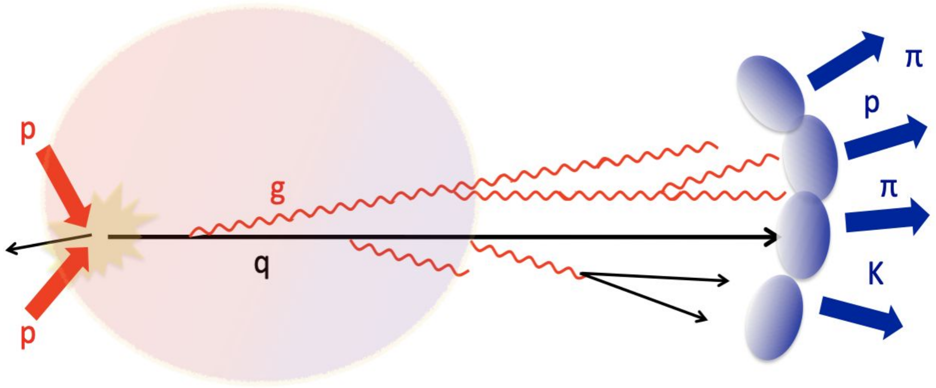

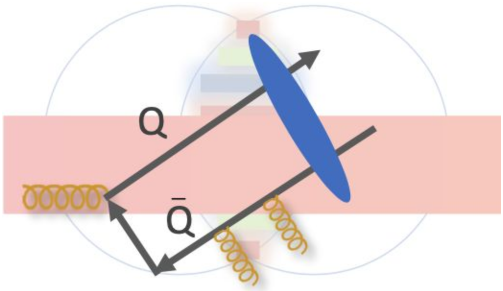

Probing the inner workings of QGP with hard (jets) or heavy (quarkonium) probes.

Jet quenching: main activity in UiB (Konrad Tywoniuk)

Quarkonium dynamics: main activity in UiS (Alexander Rothkopf)

Jet quenching: ongoing projects

Radiative processes in QGP

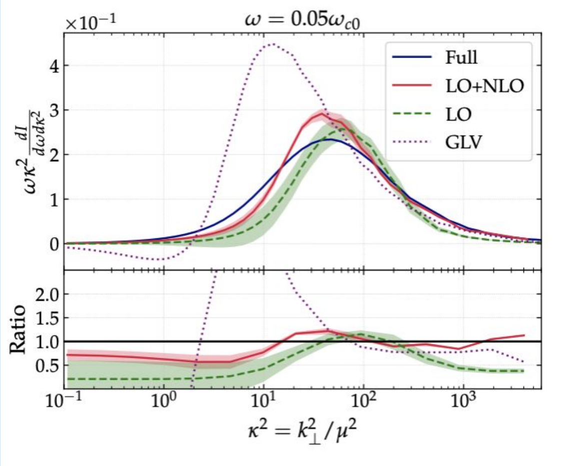

understanding jet transport parameters

Barata, Mehtar-Tani, Soto-Ontoso, KT 2106.07402

Space-time picture of jet evolution

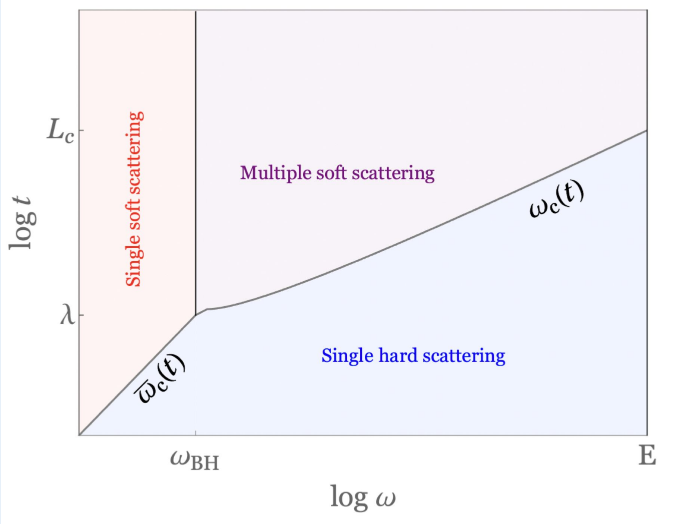

Takacs, Isaksen, KT (in preparation)

Jet quenching: ongoing projects

Full jet quenching

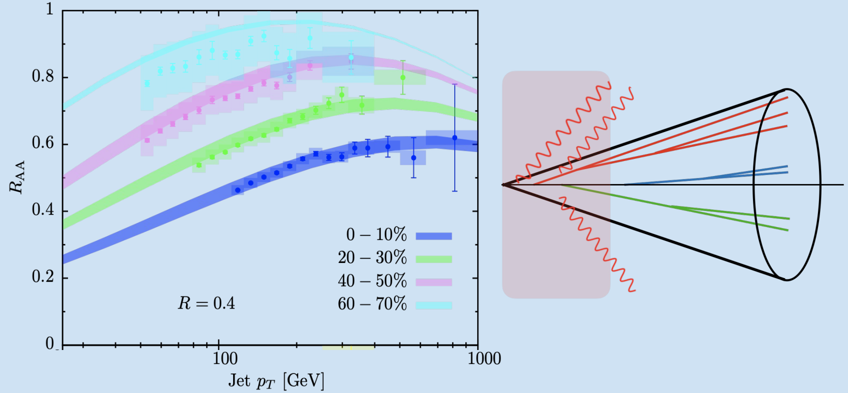

Mehtar-Tani, Pablos, KT 2101.01742
Takacs, KT 2103.14676

Jet thermalization in medium

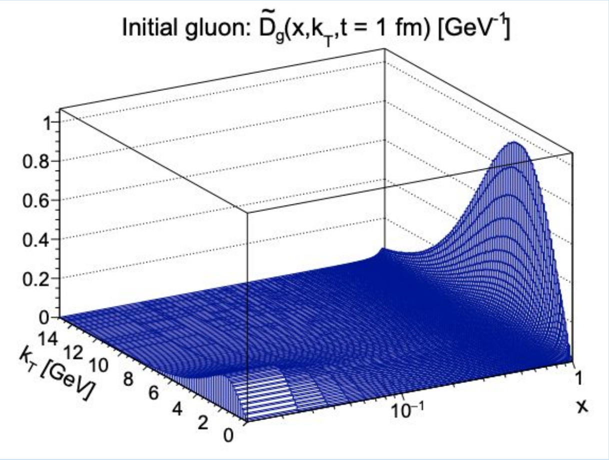

Blanco, Kutak, Płaczek, Rohrmoser, KT 2109.05918

Jet quenching: ongoing projects

Dipole shower

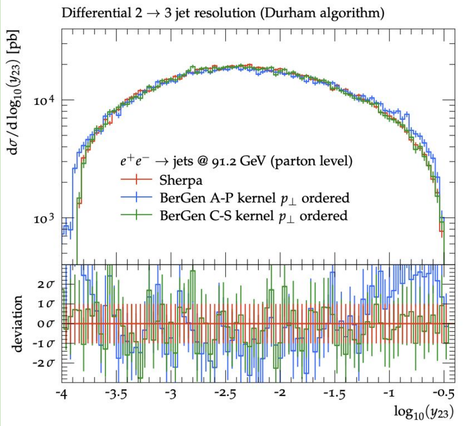

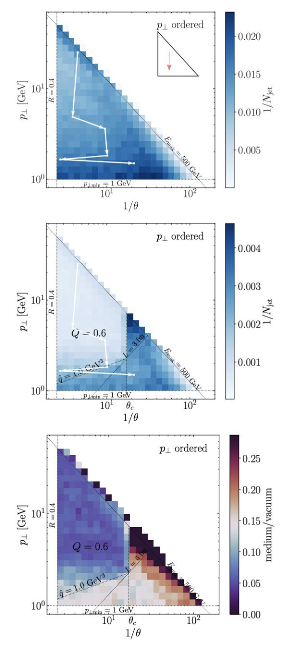

Pablos, Takacs, KT 2009.02936

Grooming & substructure techniques

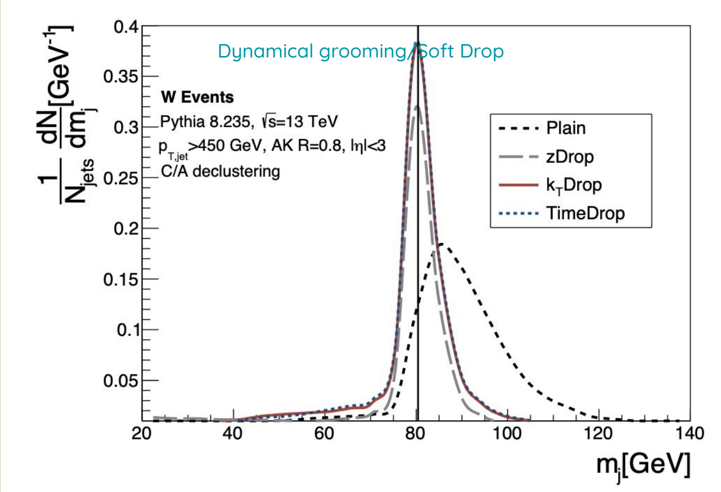

Mehtar-Tani, Soto-Ontoso, KT 2005.07584

Jet quenching: ongoing projects

Machine learning

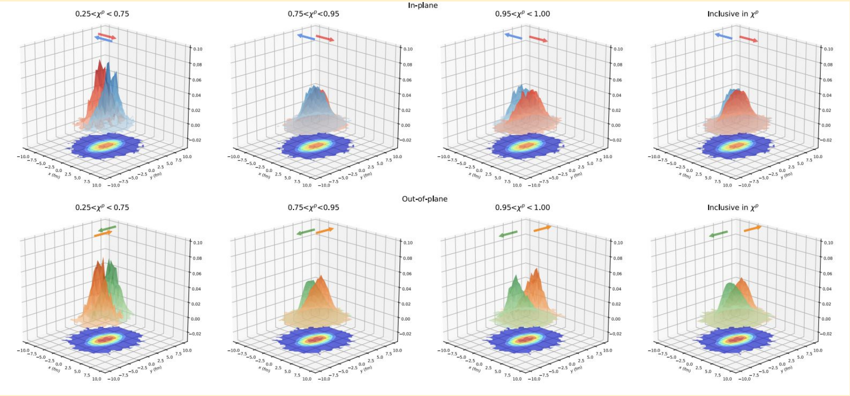

Du, Pablos, KT 2106.11271
Du, Pablos, KT 2012.07797

Bayesian inference

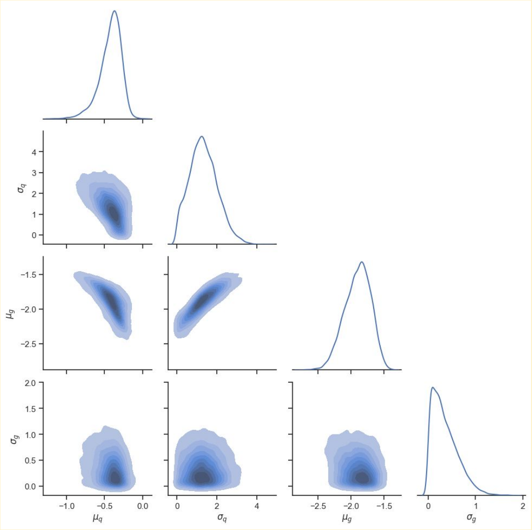

Falcao, Nielsen, KT (in preparation)

Jet quenching: future plans

Precision calculations of jet observables:

1) unified, perturbative, analytical framework
2) MC with additional non-perturbative elements
3) Bayesian, data-driven tools for designing optimal observables.

Interested in high-pT jets, substructure -> need higher statistics, more systematic searches.

Interested in small systems, connection between jet quenching & onset of hydrodynamic flow.

Quarkonium: Interested in J/ψ at high-pT (hard & heavy) - a large fraction are created in jet fragmentation.

Electron-ion: Comparison between jets (final-state radiation) and DIS (initial-state radiation) processes.

Quarkonium: ongoing projects

- Two independent approaches used to solve the singlet 1d Lindblad equation
  O. Ålund, Y. Akamatsu, F. Laurén, T. Miura, J. Nordström, A.R. JCP 425 (2021) 109917
  T. Miura, Y. Akamatsu, M. Asakawa, A.R. PRD 101 (2020) 034011

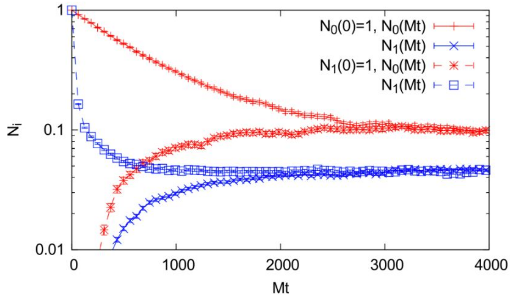

- Start either with single ground state or single excited state and monitor survival probability
- Late-time results independent of initial conditions: steady-state

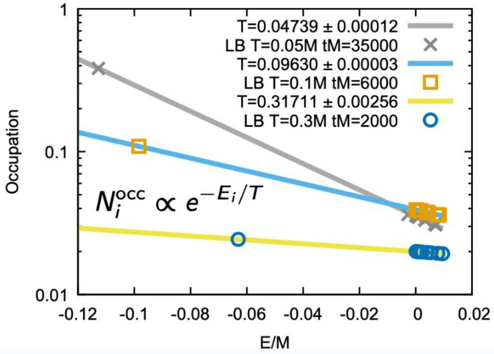

- Steady state characterized by Boltzmann distributed occupation numbers. Quarkonium temperature very close to medium temperature.
- First OQS real-time approach that can thermalize quarkonium states

Solving the 1D Lindblad equation

- Thermalization requires balance of fluctuations and dissipation.
- Naïve expectation: dissipation does not play an important role at early times

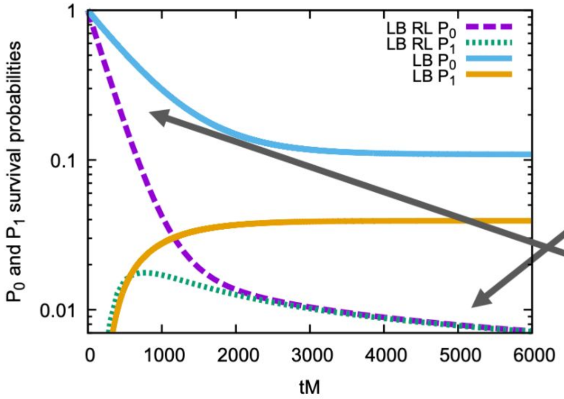

- In absence of dissipation, fluctuations heat up quarkonium system until fully randomized
- Note that dissipative effects are relevant for ground state from beginning of the evolution

- Our recent results challenge pNRQCD based OQS approaches, which do not incorporate dissipative effects and do not accommodate thermalization

Effects of dissipation

Quarkonium: plans

How to go beyond the current approximations involved in deriving the Lindblad equation, including non-perturbative effects?

Plans to restart these studies, possibly with new postdoc via Marie Curie Actions stipend.

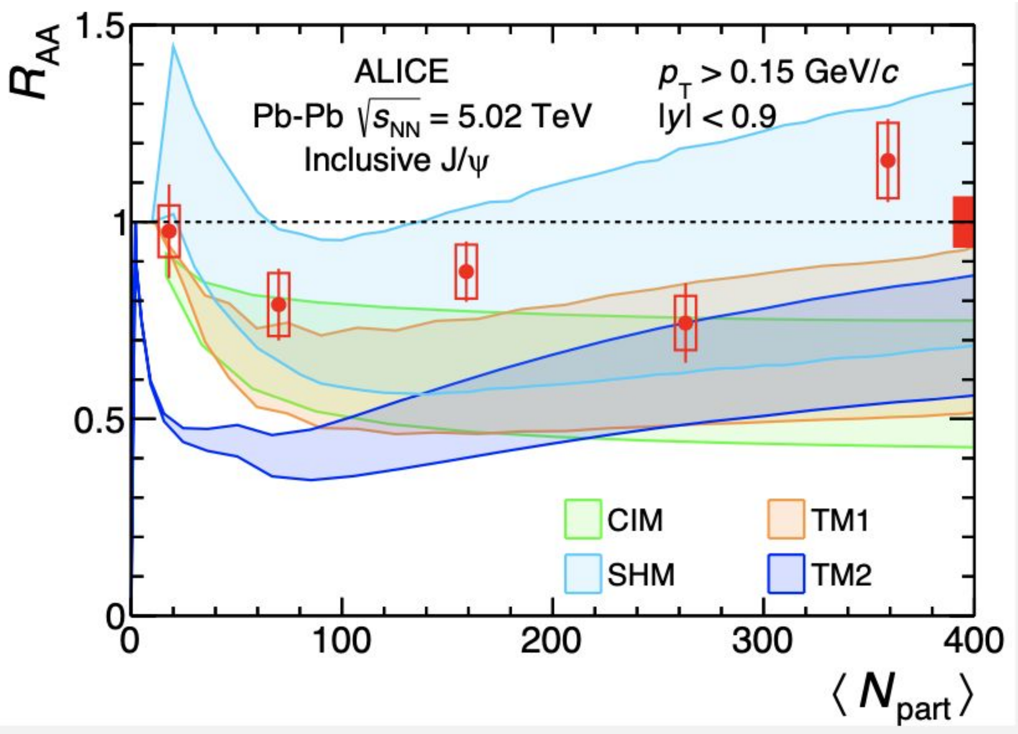

THERMAL VORTICITY AND HYPERON POLARIZATION

O.Vitiuk, L.B., E.Zabrodin, PLB803 (2020) 135298

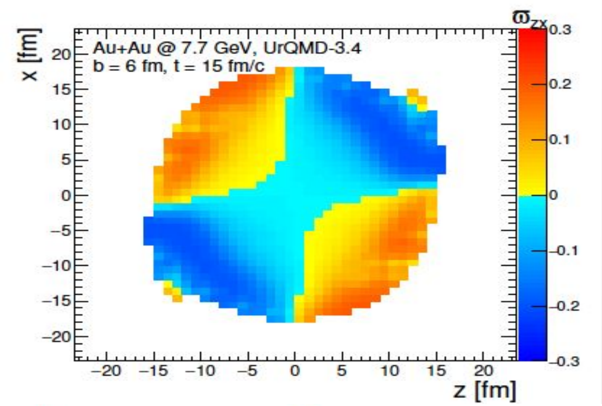

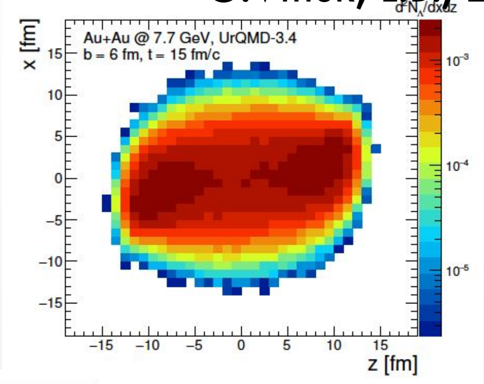

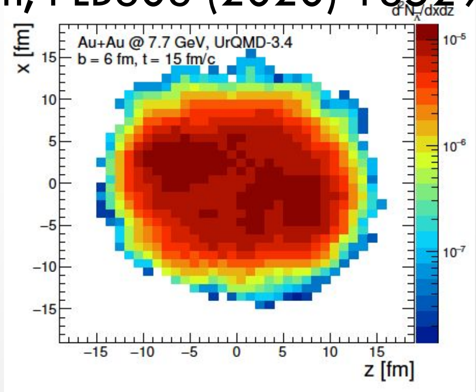

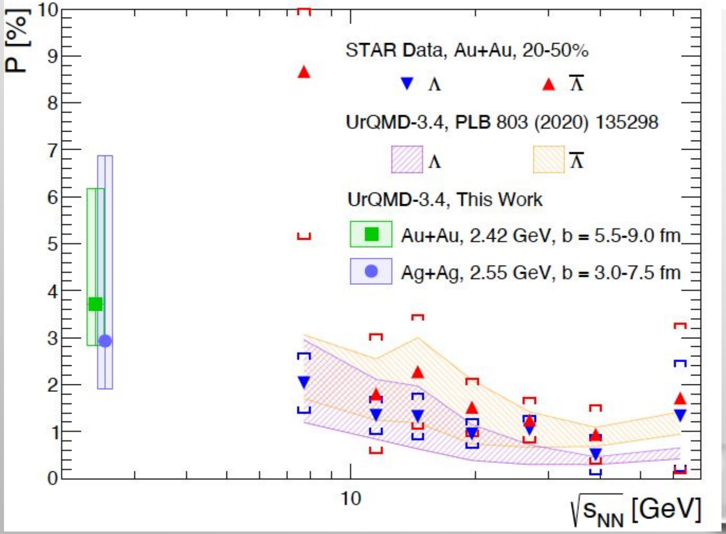

For the first time, the difference between global polarization of Λ and anti-Λ is obtained within the thermal approach. This difference is naturally explained by the difference in space-time distributions of both hyperons and different freeze-out with respect to the thermal vorticity field.

Effect of hadronic interactions on Lambda polarization
L. Csernai et al

[Y.L. Xie et al., PRC 93, 031901(R) (2017)]

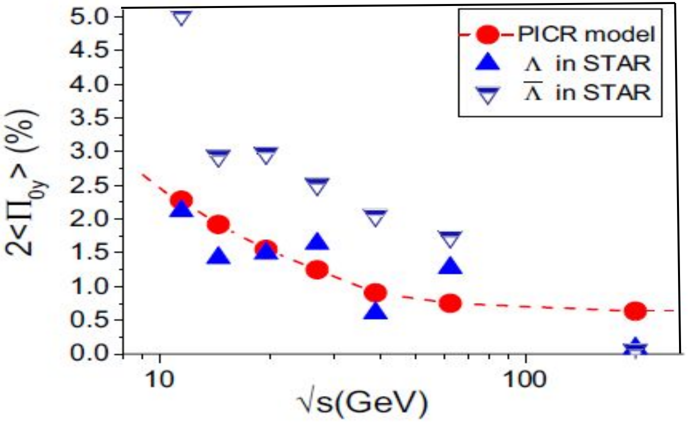

The global polarization, $2<\Pi_{oy}>p$, in our PICR model (red circle) and STAR BES experiments (green triangle), at energies √s of 11.5, 14.5, 19.6, 27.0, 39.0, 62.4, and 200 GeV.

$$< \Pi_{0y} >_p = \frac{\int dpdx \Pi_{0y}(p,x) n_F(x,p)}{\int dpdx\, n_F(x,p)} = \frac{\int dp \Pi_{0y}(p) n_F(p)}{\int dp\, n_F(p)}$$

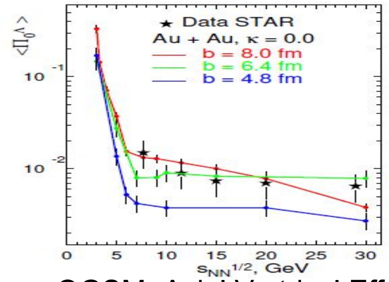

QGSM+Axial Vortrical Effect

M. Baznat, et al., arXiv:1701.00923.

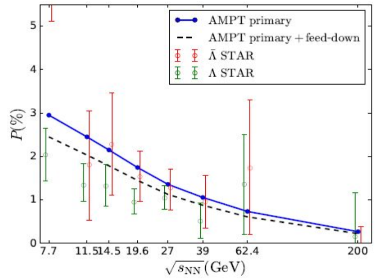

AMPT+Spin-Vorticity Coupling

H. Li, X.N. Wang et al., PRC 96,054908 (2017).

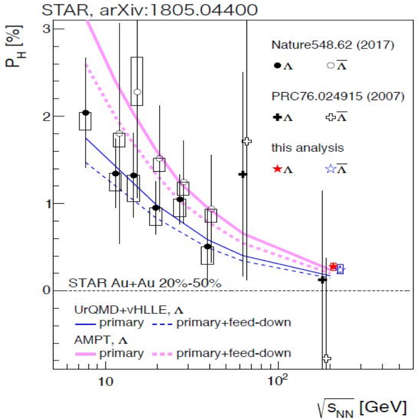

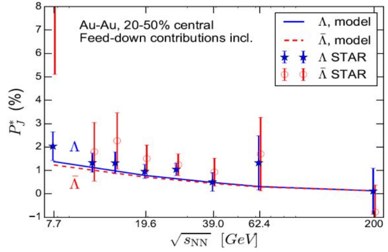

UrQMD-vHLLE hybrid Model

I. Karpenko, F. Becattini, et al., Eur. Phys. J. C 77, 213 (2017).

We use the same simulation data, but vary the freeze-out time for different collision energies.

SHEAR VISCOSITY (GREEN-KUBO METHOD)

M.Teslyk, L.B. et al., PRC101 (2020) 014904; NPA1005 (2021) 121861

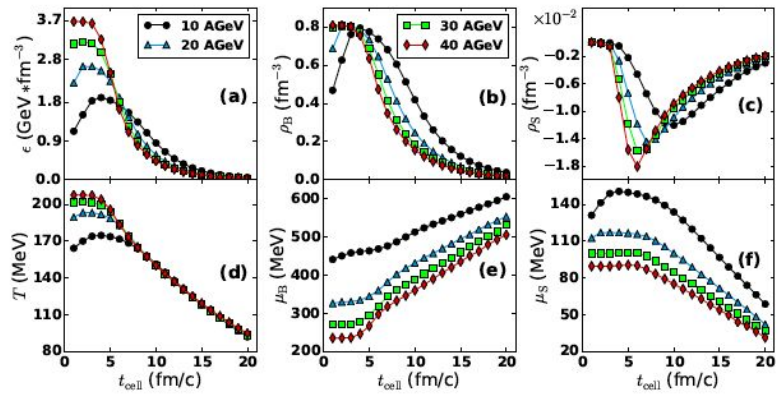

$$\eta(t_0) = \frac{V}{T}\int_{t_0}^{\infty} \langle \pi(t)\pi(t_0)\rangle_t dt$$

$$\pi^{ij}(t) = \frac{1}{V}\sum_{k=1}^{particles} \frac{p_k^i(t)p_k^j(t)}{E_k(t)}$$

$$\langle \pi(t)\pi(t_0)\rangle_t \approx \langle \pi(t_0)\pi(t_0)\rangle \exp\left(-\frac{t-t_0}{\tau}\right)$$

$$\eta(t_0) = \frac{V\tau}{T}\langle \pi(t_0)\pi(t_0)\rangle$$

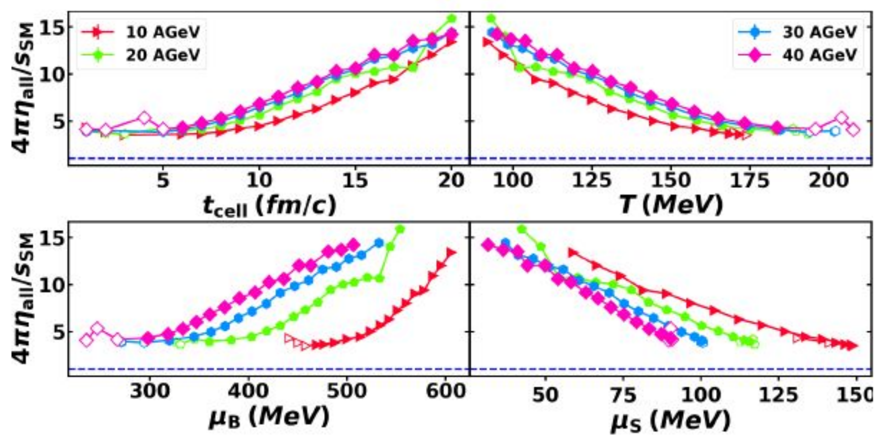

For the first time, we got the evolution of shear viscosity as function of energy density, net baryon density, and net strangeness density simultaneously.

ELLIPTIC FLOW CORRELATIONS AT LHC ENERGIES

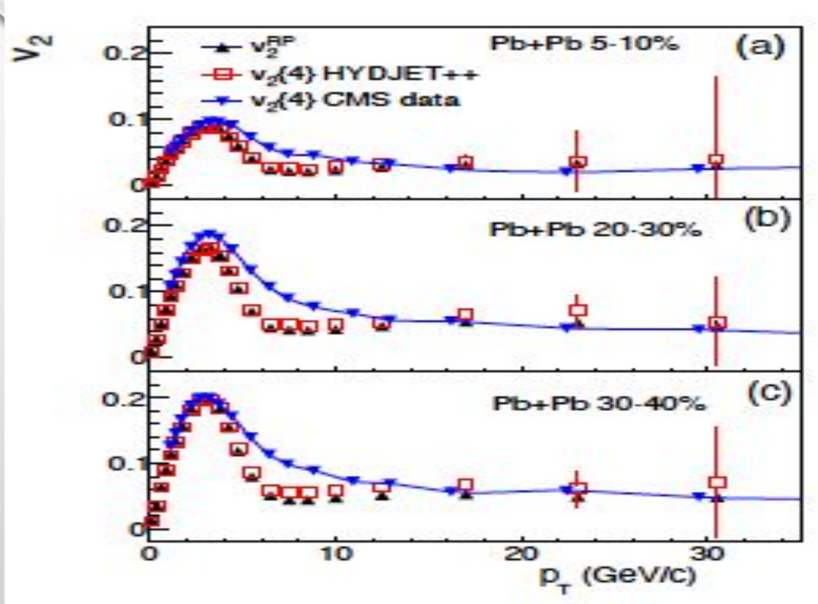

L.B., et al. PRC103 (2021) 034905

$$v_n\{2\}(p_T) = d_n\{2\} \times (c_n\{2\})^{-1/2},$$
$$v_n\{4\}(p_T) = -d_n\{4\} \times (-c_n\{4\})^{-3/4}.$$

$$c_n\{2\} = \langle\langle 2 \rangle\rangle, \qquad c_n\{4\} = \langle\langle 4 \rangle\rangle - 2 \times \langle\langle 2 \rangle\rangle^2.$$
$$d_n\{2\} = \langle\langle 2' \rangle\rangle, \quad d_n\{4\} = \langle\langle 4' \rangle\rangle - 2 \times \langle\langle 2' \rangle\rangle \times \langle\langle 2 \rangle\rangle.$$
$$\langle\langle 2 \rangle\rangle = \langle\langle e^{in(\varphi_1-\varphi_2)} \rangle\rangle, \qquad \langle\langle 4 \rangle\rangle = \langle\langle e^{in(\varphi_1+\varphi_2-\varphi_3-\varphi_4)} \rangle\rangle$$

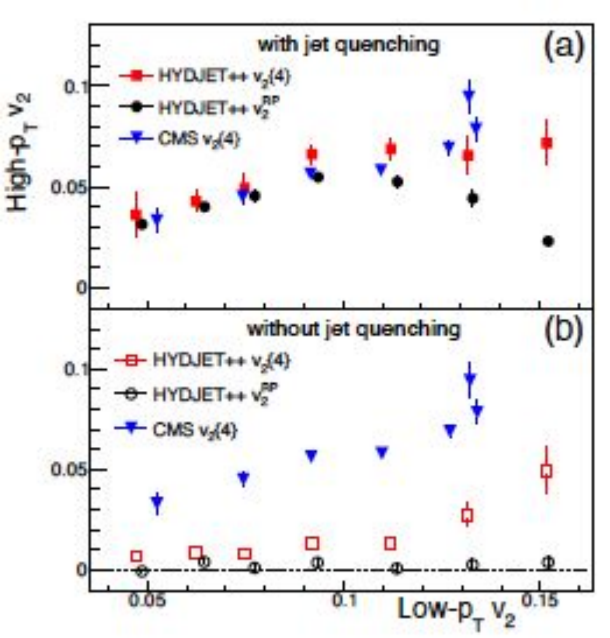

At high transverse momenta p_T > 10 GeV/c the cumulants are sensitive to both the anisotropy due to jet quenching, v^{RP} , and the particle correlations with the jet axis, v_2^{jet} . In the collisions with centrality up to 30–40% the four-cumulant method “measures” mainly the azimuthal anisotropy due to jet quenching,

CLASSIFICATION OF EOS USING DEEP LEARNING

Yu.Kvasiuk, E.Zabrodin, L.B. et al., JHEP07 (2020) 133

$$V = \sum_{i \neq j} \left(V_0^{\rm Yuk} \frac{e^{-|\vec{r}_i - \vec{r}_j|/\gamma_Y}}{|\vec{r}_i - \vec{r}_j|} + \frac{Z_i Z_j e^2}{|\vec{r}_i - \vec{r}_j|} \right) + t_1 \rho_j^{\rm int} + t_\gamma (\gamma + 1)^{-3/2} (\rho_j^{\rm int})^\gamma ,$$

$$\rho_j^{\rm int} = \left(\frac{\alpha}{\pi} \right)^{3/2} e^{-\alpha r_j^2}$$

Hard and Soft EoS

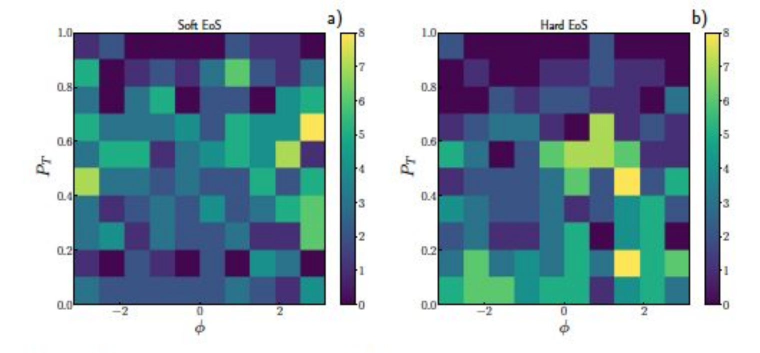

Figure 3. Proton densities for (a) soft and (b) hard potentials from a single UrQMD generated Au+Au collision at $\sqrt{s} = 11$ GeV.

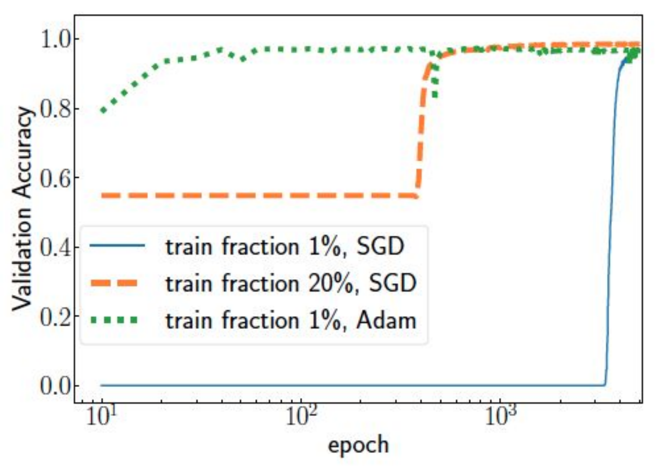

Deep Convolutional Neural Network

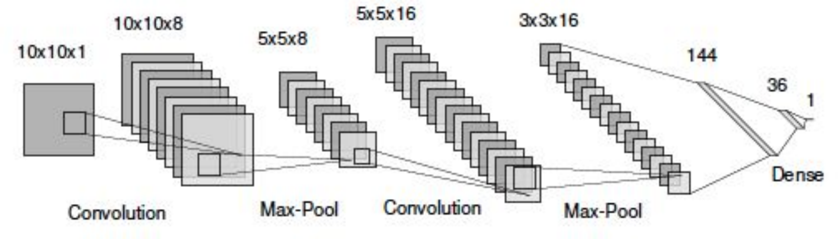

Even a small fraction of data is enough to achieve satisfactory results. Training time depends strongly on data fraction used for the training, and on the employed algorithm

The main results and topics:

1. the phenomenological transport model

PACIAE 2.2.1: An updated issue of the parton and hadron cascade model PACIAE 2.2. **Z.L. She et al., CPC 274(2022)108289**

The PACIAE 2.2.1 model is upgraded by the global chiral magnetic effect (CME)-induced initial charge separation mechanism, to mimic the CME-related physics.

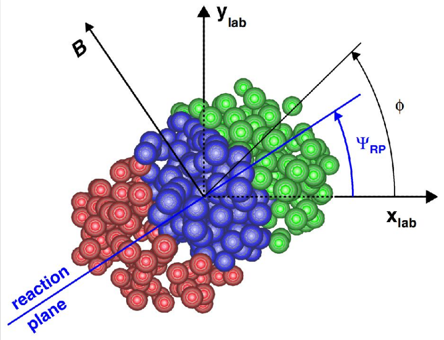

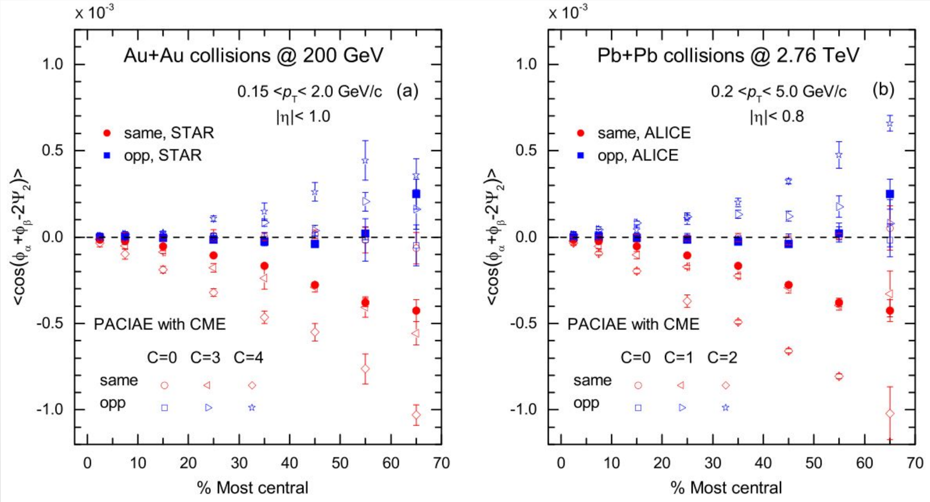

Charge azimuthal correlator γ

$$\gamma = \langle \cos(\phi_\alpha + \phi_\beta - 2\Psi_{RP}) \rangle$$

For the first time, the difference between global polarization of Λ and anti-Λ is obtained within the thermal approach. This difference is naturally explained by the difference in space-time distributions of both hyperons and different freeze-out with respect to the thermal vorticity field.

The main results and topics:

2. (Anti-)nuclei and (anti-)hypernuclei production in A+A collisions

Collision system size dependence of light (anti-)nuclei and (anti-)hypertriton production in high energy nuclear collisions. **Z.L. She et al., EPJA 58(2022)15**

The production of light (anti-)cluster in a scan of symmetric nuclear collision systems (from atomic mass number A = 10 - 238) is studied by PACIAE + DCPC model at RHIC energy; and the suppress-ion of yield ratios for (hyper)nuclei-to-hadron is also considered.

Strangeness population factor s_3 :

$$s_3 = ({}^3_\Lambda H \times p)/({}^3He \times \Lambda)$$

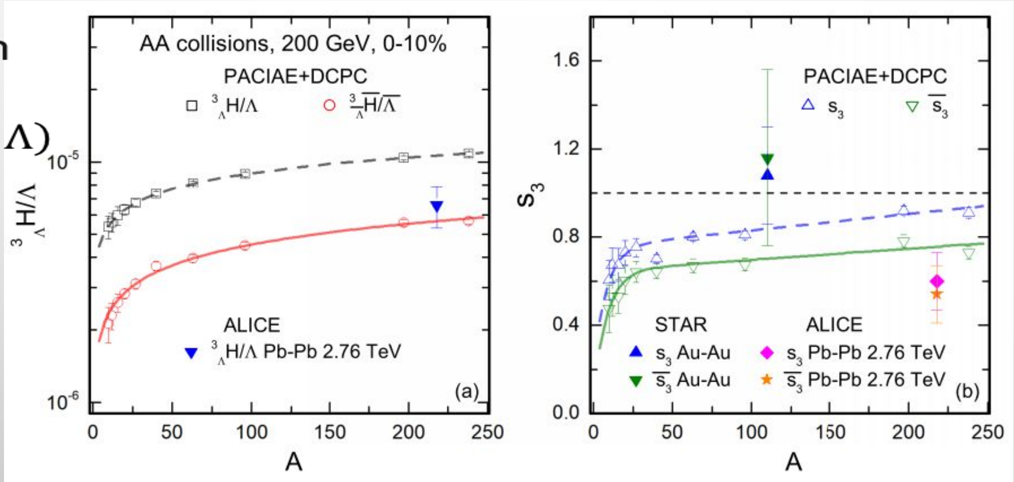

The non-smooth A dependence may be mainly related to a size effect.

The system size dependence of ${}^3_\Lambda H/\Lambda$ ratios and s_3 in different collision systems

The main results and topics:

3. Exotic states productionin high-energy nuclear collisions

   (1) Investigation of exotic state X(3872) in pp collisions at $\sqrt{s} = 7, 13$ TeV.
   H.G. Xu et al., EPJC 81(2021)784

FREEZE-OUT AND EVOLUTION OF ε AND T

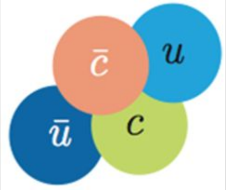

pentaquark state

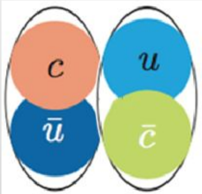

nucleus-like state

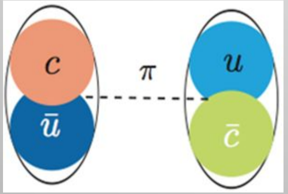

molecular state

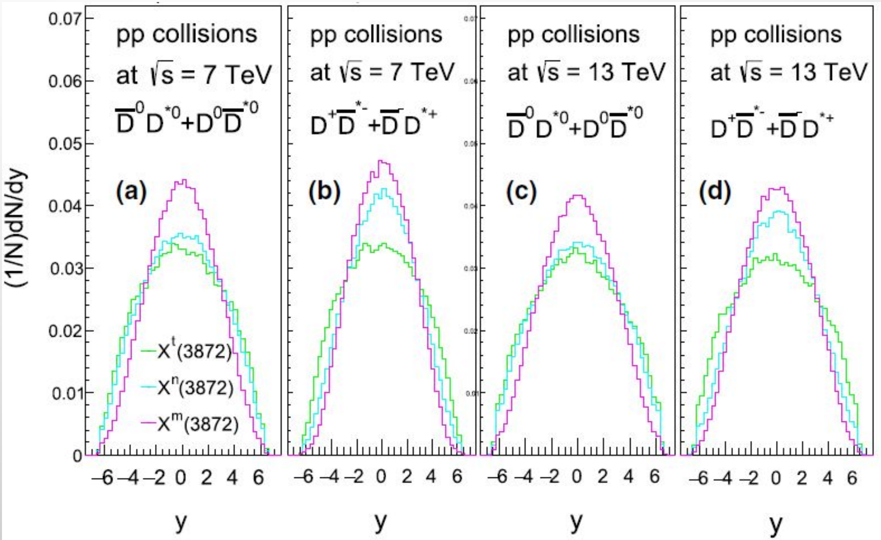

Rapidity distributions of *X(3872)* of different structures produced for different $D\bar{D}^*$ clusters in *pp* collision at $\sqrt{s}$ = 7, 13TeV

The main results and topics:

3, Exotic states productionin high-energy nuclear collisions

(2) A study on the exotic state Pc(4312), Pc(4440), Pc(4457) in pp collisions at $\sqrt{s}$ = 7,13 TeV. **C.H. Chen et al., arXiv:2111.03241. Accepted by PRD**

The exotic state Pc(4312), Pc(4440), Pc(4457) are considered to be three kinds of possible structures, i.e. pentaquark state, nucleus-like state, and molecular state based on $P_c^{\pm} \to J/\Psi p(\bar{p})$ bound state, and their productions are predicted by PACIAE+DCPC model.

Transverse momentum distribution of exotic states Pc(4312), Pc(4440), Pc(4457) with three different structures (Pcp, Pcn, Pcm) in pp collisions at $\sqrt{s}$ = 7, 13TeV

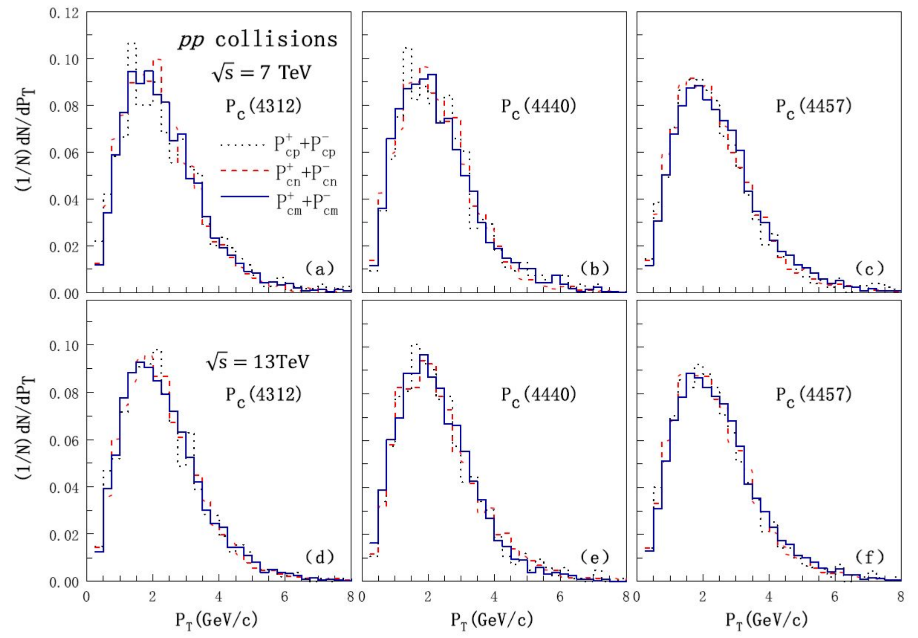

Thermal production of Sexaquarks in heavy ion collisions

Multipartonic states can be produced in enhanced way in heavy ion collisions via thermal production and coalescence mechanisms

K. A. Bugaev et al, Nucl.Phys. A970 (2018) 133-155 and references therein.

D. Blaschke, L. Bravina et al Int.J.Mod.Phys.A 36 (2021) 25, 2141005

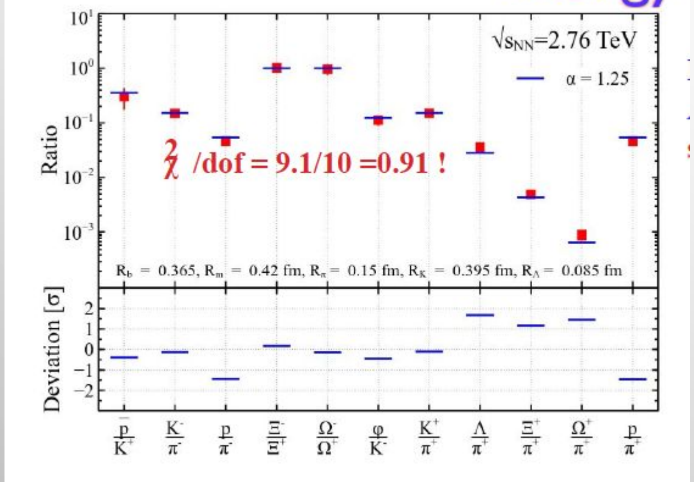

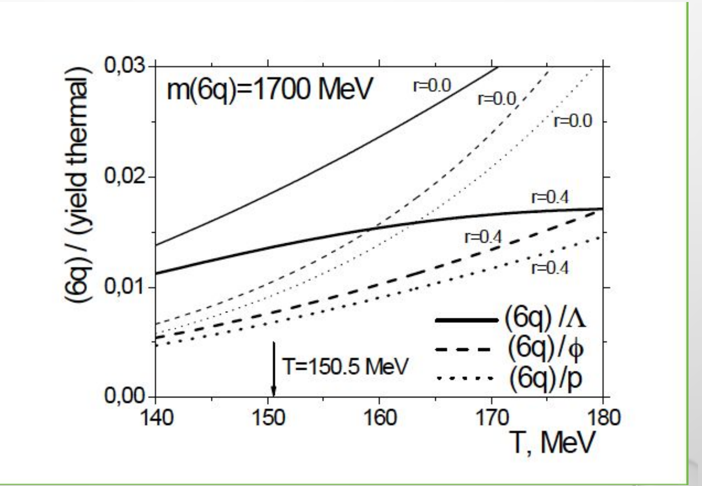

Sexaquarks are produced at relatively high rates for both 0.0 and 0.4 fm radii and for masses of 1700 and 1960 MeV
At 170 MeV the ratio of thermal Sexaquark with mass 1950 GeV to thermal deuteron ratio is about 0.45

Validation tests – Target manufacturing

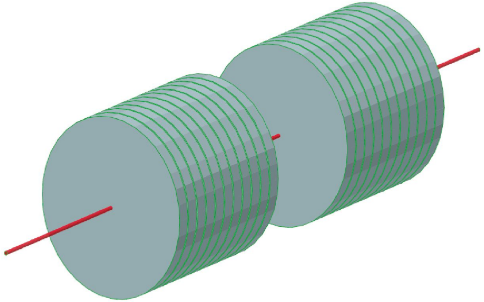

Two basic principles are tested on non-fusion material targets at low energies

- Implanted with nano-antennas Amplified absorption
- Multilayer targets Simultaneous Ignition (in progress)

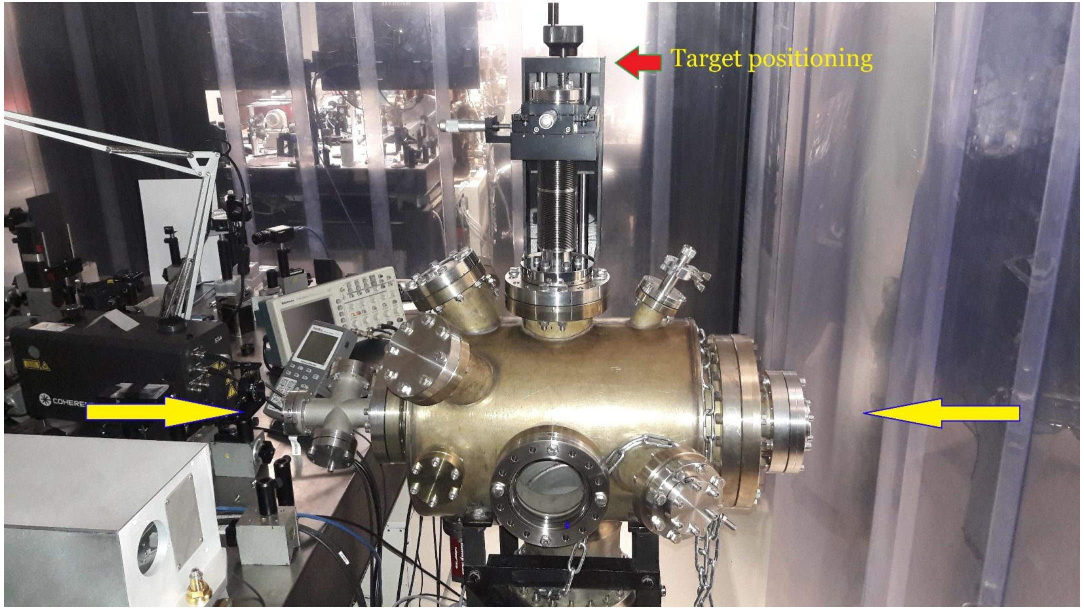

[M. Csete,
A. Bonyár,
I. Papp,
P. Rácz,
et al.]

Soon !

Future plans:

- QGSM + String Fusion Model for pp and A+A collisions
- HYDJET++ for AA collisions : flow and RAA
- UrQMD + Thermal Model for calculation of vorticity, polarisation, viscosity
- Thermal model and Coalescence model for anti-hypernuclei and exotics
  Sexaquarks
- Study of X(3872), Pc(4312), PC(4440), Pc(4457) in pp collisions at 7 and 13 TeV
  in PACIAE+DCPC model in three possible structures:
  pentaquark state, nucleus-like state and molecular state
- Machine learning
- Laser Fusion